Photochemically Implemented Metal/Polymer Nanocomposite Materials for Advanced Optical Applications

Lavinia Balan and Daniel-Joseph Lougnot
Institut de Science des Matériaux de Mulhouse,
France

1. Introduction

Nanocomposite materials metal/polymer combines together the properties of several components. Nowadays, they are regarded as promising systems for advanced functional applications (Armelao et al., 2006). In view of this, the incorporation of nanoparticles into polymer has opened the way to a new generation of materials exhibiting unique electrical, optical, or mechanical properties which make them attractive for applications in areas like optics (Jin et al., 2001; Ung et al., 2001), photoimaging and patterning (Tizazu et al., 2009; Stranik et al., 2010), sensor design (Shenhar and Rotello, 2003), catalysis (Vriezema et al., 2005), and as antimicrobial coatings (Aymonier et al., 2002; Sondi and Salopek-Sondi, 2004).

Research in novel methods to prepare metal nanocomposite materials has been greatly stimulated due to their attractive properties and promising applications. One of the main interests of metal nanoparticles stems from their unique physical properties which can be addressed by the chemical control of their shape and size (El-Sayed, 2001; Eustis and El-Sayed, 2006). Amongst them, gold, silver and cooper with nanometer size, have been the focus of great interest because these nanoparticles exhibit a very intense absorption band in the visible region due to their surface plasmon resonance.

Metal/polymer nanocomposites can be prepared by two approaches. The first one involves metal nanoparticles dispersion in a polymerizable formulation, or in a polymer matrix. In this case, the reduction of metal ions and polymerization occur successively hence the aggregation of nanoparticles that makes this synthetic procedure often problematical. In the second approach, nanoparticles are generated in situ during the polymerization to avoid agglomeration. The polymerization reaction and the synthesis of nanoparticles that proceed simultaneously were the subject of extensive studies.

Another technique consists in polymerizing the matrix around a metal nanocore by using chemically compatible ligands (Mandal et al., 2002) or polymeric structures (Corbierre et al., 2001).

In all cases, the high-performance of nanomaterials depends on the controlled distribution of uniformly shaped and sized particles. Therefore, the development of synthetic strategies to control particles growth and/or agglomeration during nanocomposite fabrication appears quite obviously as a key challenge.

Photochemical reduction by irradiating a dye sensitizer in the presence of metal ions provides a convenient way to produce nanoparticles embedded in polymer (Balan et al.,

2008; Korchev et al., 2004; Sangermano et al., 2007; Sudeep and Kamat, 2005; Yagci et al., 2008). In this context, the photoinduced synthesis has many advantages since it combines the characteristic features of light activation i.e. versatility and convenience of the process, high spatial resolution and reaction controllability (intensity and wavelength), with the simplicity of the colloidal approach. Various photo-induced synthetic strategies to obtain metal nanoparticles in a variety of conditions have been described by Sakamoto et al. (Sakamoto et al., 2009). However, photoassisted processes allowing the generation of polymer/metal nanocomposites that were introduced very recently are still in demand of further investigation.

2. Materials and methods

The absorption spectra were recorded using a Perkin-Elmer Lambda 2 spectrophotometer. Photochemical reactions were carried out under irradiation at 532 nm with a cw laser VERDI from Coherent. The progress of the reactions was monitored via UV-Vis absorption spectroscopy.

Photopolymerization kinetics was studied in situ by real-time FTIR with an AVATAR 360 spectrometer from Nicolet. The formulation was sandwiched between two polypropylene films (10 µm thick), deposited on a BaF2 pellet. Flood exposure during FTIR measurements was performed using a laser diode (type Cube from Coherent) emitting at 532 nm with an average intensity 5 mW/cm². The conversion rates were deduced from the progressive disappearance of the vinyl C=C stretching vibration band at 1630 cm^{-1}. Rp – the rate of polymerization - is defined as the maximum of the first derivative of the conversion vs. time curves. Usually, it is measured at the early time of the polymerization when the monomer concentration remains close to the initial bulk concentration ($[M]^0$)

For recording holographic gratings, a typical setup of four-wave mixing based on a frequency-doubled cw YAG laser emitting at 532 nm (s-polarization) described earlier was used (Lougnot and Turck, 1992; 2002). The two arms of the interferometer were equipped with a spatial filter and the fringe visibility could be set with the help of a polarizing beam splitter and a system of half-wave plates. A low-intensity He-Ne laser beam ($\lambda = 633$ nm, 0.5 mW) placed at the Bragg angle corresponding to the spatial period of the grating, was used for real-time monitoring of the grating formation. The diffraction efficiency was calculated as $\eta = I_{Diff} / (I_{Tr} + I_{Diff})$ where I_{Tr} and I_{Diff} are the intensities of the transmitted and first order diffracted beams, respectively.

A specific device was developed to characterize holograms. It allows the record to be interrogated by a reading laser diode emitting at 633 nm with incidences covering a ± 10° angular window on both sides of the Bragg incidence. The curve showing the actual diffraction efficiency as a function of Δθ' exhibits the well-known squared cardinal sine shape. It was thus, possible to use the Kogelnik's (Kogelnik, 1969) relationship for further calculation of the modulation of refractive index (Δn) and the effective thickness of the gratings (d).

The light energy needed for the input and output of the necessary information depends on the efficiency of the holographic recording material. The holographic sensitivity means a quantity inverse to the input energy (or energy density) at which the necessary output signal level appears (Collier et al., 1971). In a way, it measures the build up rate of a hologram. If the visibility is assumed to equal unity, the holographic sensitivity per unit area G (in cm²/J) expressed as follows (Carré and Lougnot, 1990):

$$G = \eta^{1/2} / I_0 t \qquad (1)$$

where I_0 is the power density in the two beams and t, the holographic exposure.

Transmission electron microscopy (TEM) was used to characterize the size and shape of Ag nanoparticles. Samples were sliced down by means of a microtome (LKB model 8800) and placed onto the copper grid. TEM measurements were carried out using a Philips CM20 instrument with LaB6 cathode. The gratings were also examined by a FEI 400 Scanning electron microscopy (SEM) and an atomic force microscopy (AFM) using a Pico Plus instrument from Molecular Imaging. After disassembly of the samples, the free surfaces of the records were analyzed in tapping mode with a Si_3N_4 tip the resonance frequency and spring constant of which were 100 kHz and 0.6 Nm^{-1}, respectively.

The precursor of metal nanoparticles was silver nitrate (ACS Reagent 99 % from Aldrich). It was added to the formulation as a fine powder and upon stirring, one hour before use. The formulations used in this work contained a liquid acrylic multifunctional monomer (typically, pentaerythrytol triacrylate, PETA from Cytec, Polyethyleneglycol 400 diacrylate, SR 344 from Sartomer and/or Bis-phenol A diacrylate, Ebecryl 600, from Cytec). The initiating system was based on a photosensitizer absorbing in the yellow-green range (Eosin Y) and an electron donor (methyldiethanol amine – MDEA - or ethyl-2-dimethyl amino-4-benzoate – EDMAB). These products were purchased from Sigma Aldrich and used as received.

The precursor of sol-gel materials was 3-[(MethAcryloxy)Propyl] TriMethoxySilane (MAPTMS). It was purchased from Aldrich and used as received.

3. Results and discussion

The present work reports a strategy to produce a nanoparticles-embedded polymer through a photoinduced one-step one-pot method. In this approach, a system combining a visible photosensitizer - Eosin Y dye (Scheme 1) and an electron donor - N-methyl diethanolamine (MDEA) was used to photogenerate Ag nanoparticles and to photoinitiate the free radical polymerization of a multifuctional acrylate monomer.
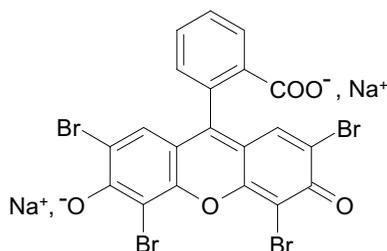
Scheme 1. Structure of Eosin Y disodium salt

Compared to the prior state of the art, the major innovation lies in the use of visible light to initiate both polymerization of the monomers and reduction of the metal nanoparticles precursor (silver cations) at the same time (Balan et al., 2008; 2010).

In short, this mechanism involves:

i.   the photogeneration of amine-derived initiating radicals (Amine•+),
ii. the reduction of silver cations by the aminyl radical produced by the previous reaction,

iii.   the initiation of radical polymerization of the monomer binder.

$$Sens\ +\ h\nu\ \rightarrow\ Sens^*$$
$$Sens^*\ +\ Amine\ \rightarrow\ Sens^{\bullet-}\ +\ Amine^{\bullet+} \qquad (i)$$
$$Amine^{\bullet+}\ \rightarrow\ Amine^{\bullet}\ +\ H^+$$
$$Amine^{\bullet}\ +\ Ag^+\ \rightarrow\ X\ +\ Ag_0 \qquad (ii)$$
$$Amine^{\bullet}\ +\ Monomer\ \rightarrow\ Living\ polymer\ radical^{\bullet} \qquad (iii)$$
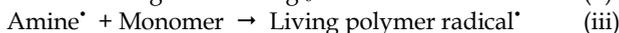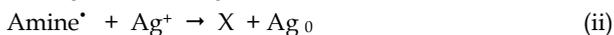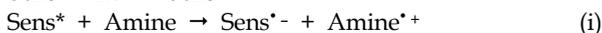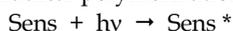
3.1 Fabrication of silver nanoparticle embedded polymer

A formulation of SR 344 – 80 % and E 600 – 20 % monomers containing Eosin Y (0.1 wt %), MDEA (3 % wt) and $AgNO_3$ (1 wt %) was photopolymerized upon irradiation at 532 nm (2.5 mW cm^{-2}). The conversion of acrylate double bonds was monitored from the decrease of the IR band at 1630 cm^{-1}. The conversion rate of this formulation was compared with that of a reference sample without $AgNO_3$ (Figure 1). Both samples show a similar rate of polymerization (within experimental error limits) with a maximum conversion degree leveling off at ca 80 %. This well-known effect is due to the crosslinking process. In fact, high crosslink density results in a gel-effect and the entanglement of living polymer chains sets a limit to the extent of conversion (Mehnert et al., 1997).
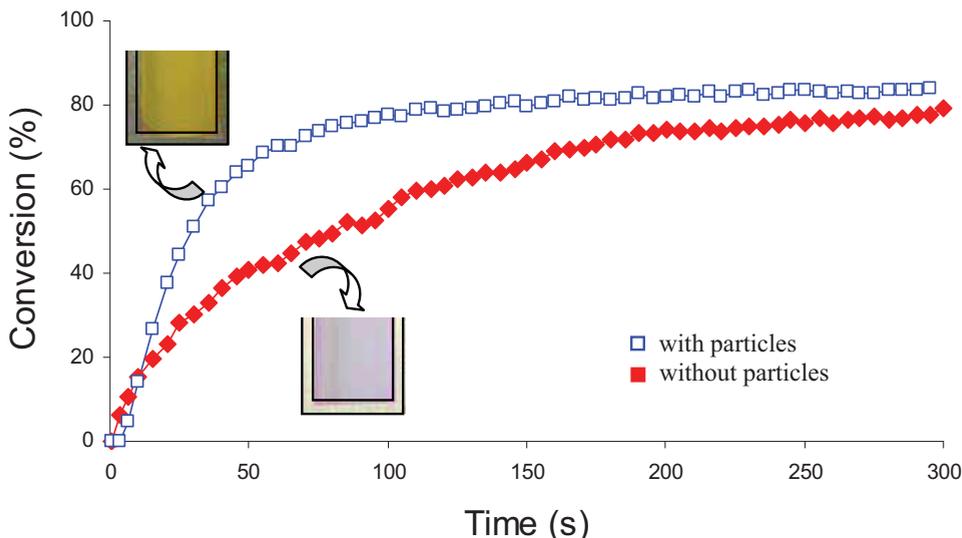

Fig. 1. Real-time FTIR kinetic conversion curves for visible curing at 532 nm of resins with and without particles (Insets: View of 30 µm thick samples with and without nanoparticles after curing)

It is worth of notice that addition of Ag^+ did not perturb the photopolymerization kinetics (Figure 1). On the contrary, the in situ synthesis of silver nanoparticles concomitantly with the photopolymerization process was observed to have an unexpectedly favourable effect on the rate of polymerization (Rp) (for instance, after a 100 s exposure, the conversion ratio are 55% and 80% in the absence and in the presence of nanoparticles, respectively). In the presence of metal nanoparticles, the polymerization started after a short inhibition period (ca 5 s), the conversion leveled off at a slightly higher value (83 % instead of 75 %) and above all, the Rp

was accelerated by a factor of 1.9 (in the presence of metal nanoparticles Rp is 2.6 M.l^{-1}.s^{-1} and without particles, 1.4 M.l^{-1}.s^{-1}). Therefore, the generation quantum yield of MDEA$^{\bullet}$ was sufficiently high to enable both free radical photoinitiation and photogeneration of Ag nanoparticles. Moreover, after 5 min exposure, the reference sample turned from pink to colourless whereas the sample with Ag$^+$ turned from pink to yellowish (inset Figure 1).

The absorption spectrum of the sample underwent important changes during visible irradiation (Figure 2). The absorption band of EO^{2-} faded off progressively while the surface plasmon resonance developed in the 350-500 nm region. This band exhibited a maximum wavelength at 437 nm with a FWHM of ca 115 nm.
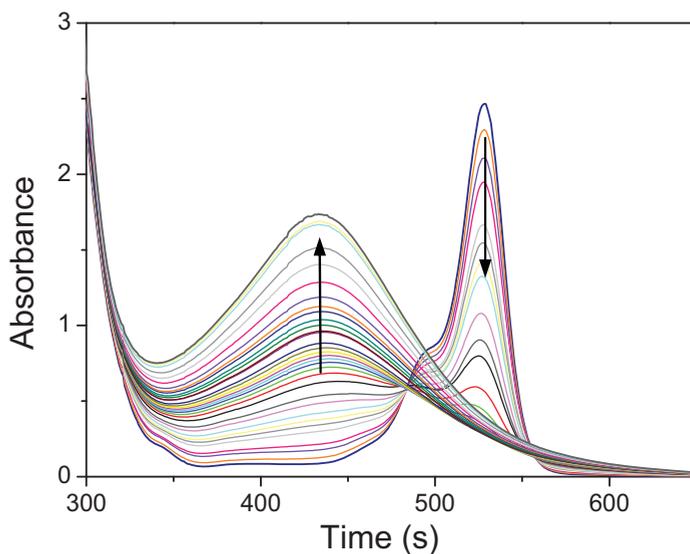

Fig. 2. Time evolution of the absorption spectrum of the resin during photopolymerization EO^{2-}/ MDEA / AgNO$_3$, (0.1 / 3 /1 wt %)

Careful analysis of the absorption spectrum over the illumination period clearly reveals a process corresponding to the photobleaching of EO^{2-} with the concomitant growth of the surface plasmon band.

The bright field TEM micrograph of a silver-nanocomposite is shown on Figure 3. Throughout the photoreduction process, the symmetrical shape of the surface plasmon band denotes a very narrow size-distribution of the silver nanoparticles photogenerated in the polymer matrix.

Electron microscopy analysis of the nanocomposite material confirmed the formation of monodisperse spherical metallic particles in the nanometer range size. Analysis of a population of ca. hundred particles from a portion of the grid indicated that their average diameter was 5.0 ± 0.7 nm. They were homogeneous in size and no agglomeration was observed. Such a homogeneous distribution can be accounted by the stabilizing effect of the monomer matrix. Through its acrylate functions, the monomer can easily adsorb on the nanoparticle surface. In this respect, the capping effect of unsaturated long-chain agents was previously reported by Wang et al. (Wang et al., 2002), who correlated the size of silver particles with the number of available double bonds in the chain.
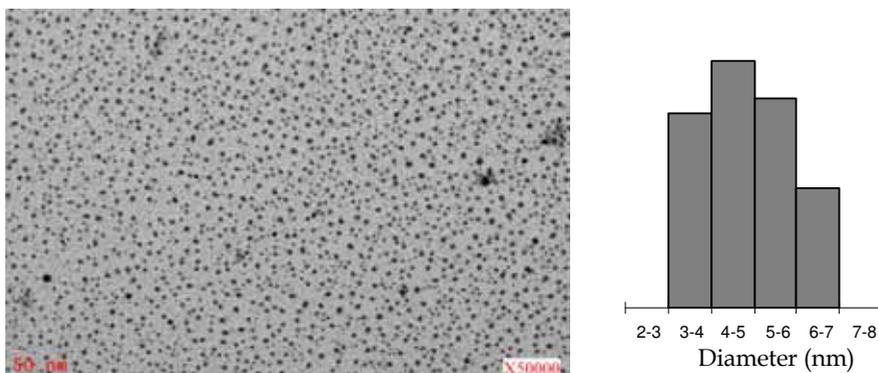
Fig. 3. TEM image of silver nanoparticles embedded in a polyacrylate matrix, with the corresponding size distribution

3.2 Silver /hybrid sol-gel nanocomposite

Polymer matrixes suffer from intrinsic limitations due to the physical properties of the material: low refractive index, poor mechanical and thermal properties, dewetting or delamination effects limiting their use as thin films.

In this context, the sol-gel approach has proved to be an interesting alternative whenever the nanocomposite is to be used as a thin film coating (< 1µm). Indeed, the presence of SiOH moieties favours adhesion of the film onto substrates such as Si or SiO_2 and the stabilization of nanosized metal particles.

Moreover, special attention has been paid to photopolymerizable hybrid sol-gel materials (Soppera and Croutxé-Barghorn, 2003.) since they allow the formation of hybrid organic-inorganic materials by acid- or base-catalyzed hydrolysis and condensation of main group or transition metal alkoxides (Judeinstein, 1996). Due to the presence of a photopolymerizable function covalently bounded to the inorganic part, the specific advantages of photocuring are preserved: low temperature processing and spatial control of the polymerization reaction for photolithographic applications (Kärkkäinen, 2002).

The photochemical one-pot and one-step process was used in a hybrid sol-gel formulation to synthesize silver nanoparticles (Scheme 2), thus combining the advantages of the photochemical route to prepare nanocomposite materials with the unique properties of hybrid sol-gel matrix.

Silver particles/sol-gel nanocomposites films with open surface were prepared by photoinduced reduction of $AgNO_3$ and photopolymerization of a hybrid sol-gel host medium. Such highly crosslinked hybrid sol-gel films containing well-dispersed silver nanoparticles should arouse much interest in the world of optical waveguiding and coatings because of the potential of these new materials. Moreover, ultra-thin films of silver/sol-gel nanocomposites open new prospects in biomedicine and optoelectronics.

3.3 Applications of silver/polymer nanocomposites
3.3.1 Holographic recording

Holographers are in permanent demand for recording materials with more and more sophisticated technical features that justifies their great interest for metal/polymer nanocomposites. Furthermore, the development of periodically ordered metal structures

should open up new vistas because of the possibility to couple propagative lightwave and surface plasmons, a promising field of research and development for designing diffractive optical elements with ultrahigh spectral dispersion (Mikhailov et al., 2007). And finally, the possibility to generate strings of metal nanoparticles embedded in a polymer matrix through a photochemical process that allows them to be manipulated seems to arouse much interest in the plasmonics community.
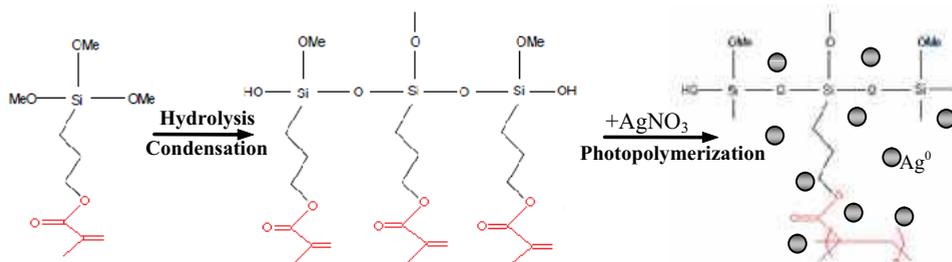
Scheme 2. Formation of silver /hybrid sol-gel nanocomposite

As regards holographic materials for storage applications, the introduction of an additional neutral component within the reactive formulation is a recurring concern for those who are developing new recording systems. It is based on the counter-diffusion of the components of the holographic formulation between the bright and dark regions under the influence of gradients of chemical potential induced by the photopolymerization of monomers. In the search for more and more innovative systems, Vaia et al. pioneered the use of nanoparticles (inorganics, organic polymers, metals or metal oxides) (Vaia et al., 2001). High diffraction efficiencies were reported in polymerizable blends containing nanoparticles (metals or oxides) synthesized beforehand (Nakamura et al., 2009; Sanchez et al., 2005). However, dispersing the nanoparticles in the reactive formulation was always mentioned as a critical step in the process.

Recently, the synthesis of new nanocomposites containing functionalized monomers and Au nanoparticles coated with ethyl 11-mercaptoundecanoate that allowed refractive index modulations exceeding 0.007 (i.e. diffraction efficiencies of ca 50 % in 20 μm films) was reported (Goldenberg et al., 2008). The mechanism of refractive index contrast amplification in this new material was claimed to include both segregation of the components due to photoinduced gradients of concentration and interception of free radicals by Au nanoparticles. In contrast, and in spite of many works of scientists involved in this field, efforts aimed at fabricating spatially organized metal-polymer nanocomposites by an all-photochemical process were inconclusive and only weak diffraction efficiencies were reported.

Following the line of the one-pot one-step synthesis of metal/polymer nanocomposites described before, the holographic recording properties of acrylate formulations containing silver nanoparticles photogenerated in situ were investigated.

A formulation containing SR 344 (80%) and E 600 (20%) was used to record holographic gratings. The concentration of the sensitizer was adjusted so that the optical density of the samples was ca 0.6 at maximum (typ. 3×10^{-3} M). The holographic samples were sandwiched between two glass slides (28 x 76 mm) separated by a calibrated wedge. The thickness of the samples was either 23-24 μm or 45 μm, depending on the wedge used. The polymerizable formulations were prepared 24 hours before use and stored at room temperature in dark conditions.

According to the theory of holography, the gratings with spatial periods of ca 1 μm and thickness of 16 or 30 μm are Bragg volume gratings (Collier et al., 1971) only 0 and -1 orders were observed in the diffraction pattern. The angular dependence of the holographic response of the gratings showed excellent agreement with the Kogelnik analysis for thick phase gratings (Kogelnik, 1969).

An example of holographic sensitivity curves without and with silver nanoparticles is shown on Figure 4. The holographic sensitivity and efficiency at maximum of the gratings and the refractive index modulation achieved are presented in table 1 as a function of the recording conditions.

In this work, the reference system was deliberately selected because of its poor recording performances. It is characterized by a limited potential in terms of available index modulation that is related to the use of a mixture of two acrylic difunctional monomers and a tertiary amine generating EDAB-derived aminyl radicals that are reputedly mediocre initiators of polymerization (Pyszka and Kucybała, 2008). In such a formulation, the fate of silver nanoparticles is to undergo spatial segregation under the influence of driving forces resulting from differences of local properties between dark and bright fringes. Amongst the possible causes for this segregation, one can mention gradients of photoreduction rate of silver cations or gradients of crosslinking degree of the monomers, that both replicate the spatial distribution of the actinic light in the incident interference pattern.
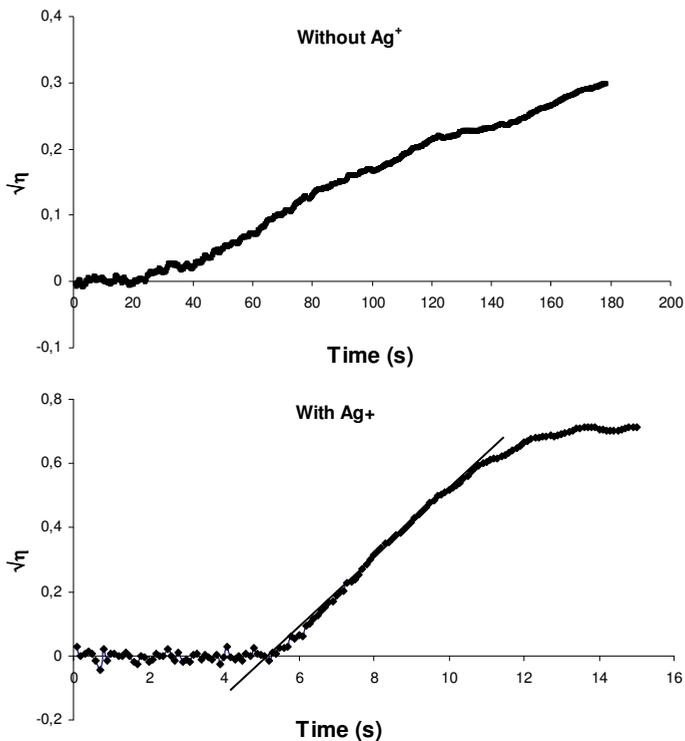

Fig. 4. Holographic sensitivity curve derived from holographic recording results of sample 1 without Ag^+ (a) and sample 3 with 1% w/w Ag^+ (b) in Table 1 with the model of eq. (1)

A dramatic improvement of the recording characteristics of the formulation containing silver cations was observed. The amplitude of the available modulation of refractive index was much larger while the holographic sensitivity increased up to a hundredfold with $[Ag^+]$ = 1 % w/w. There is no doubt that the presence of silver nanoparticles photogenerated in situ is the key factor that is behind the change in the recording properties. However, it is worth of notice that a twofold increase of the concentration in silver cations did not improve the recording process further: the holographic efficiency increased by some 20 % while η_{max} decreased slightly.

The results reported in table 1 reveal also the influence of both the chemical and photonic parameters on the diffraction efficiency at maximum and the holographic efficiency (Balan, 2009). In the presence of silver, addition of increasing amounts of coinitiator (EDMAB) results in an important acceleration of the recording process. This observation is mainly accounted for by the increase of the photoreduction quantum yield of Eosin in its triplet state by EDMAB (Noiret et al., 1994).

Sampe	EDMAB (M)	Ag+ (% w/w)*	Total fluence (mW/cm²)	Exposure (s)	η_{max} (%)	Δn (x 10⁻⁵)	G (cm²/J)
1	0.4	0	20.8	180	8.9	121	0.13
2	0.4	0	41.8	240	16.9	185	0.12
3	0.4	1	10.0	60	52.7	290	12.2
4	0.4	1	10.0	15	41.1	265	12.3
5	0.2	0.5	5.0	150	68.1	308	4.2
6	0.2	0.5	10.0	100	69.2	303	3.9
7	0.2	0.5	20.0	60	80.0	376	2.8
8	0.2	1	10.0	60	48.7	300	4.8
9	0.2	1	20.0	30	72.5	329	3.6

(*) 0.5% w/w = 0.024 M; 1 % w/w = 0.059 M

Table 1. Influence of the chemical and photonic parameters on the holographic sensitivity, diffraction efficiency at maximum of the gratings and refractive index modulation

Table 1 shows also that increasing the recording fluence always goes along with an increase of the diffraction efficiency at maximum but also with a decrease of the holographic efficiency. This behaviour is to be interpreted in terms of coupling between chemical reactions generating active species involved in the modulation of refractive index and physical processes responsible for the segregation of the components of the holographic formulation. The higher the fluence used to record the holographic grating, the faster the recording process but the less efficient is the segregation process (Samui, 2008).

Since the concentrations of Ag^+ used in this work were quite small, the increase of refractive index modulation cannot be only accounted for by the presence of silver nanoparticles. Clearly, indirect physical and chemical effects of the nanoparticles must be invoked. Due to their strong interaction with nucleophilic groups, they are able to modify the polymerization kinetics and as an indirect consequence, the composition and morphology of the copolymer formed at the local scale. Given the difference of chemical structure and refractive index between the comonomers used (n_{E600} = 1.548 and n_{SR344} = 1.466), only a 1 %-modification of the copolymer composition between bright and dark areas of the record induces an increase of refractive index modulation of ca 150 10⁻⁵.

Analysis of the records by AFM, SEM and TEM

AFM

Figure 5 shows the AFM characterization of two samples obtained with formulations without particles and with 1% w/w Ag⁺, respectively.
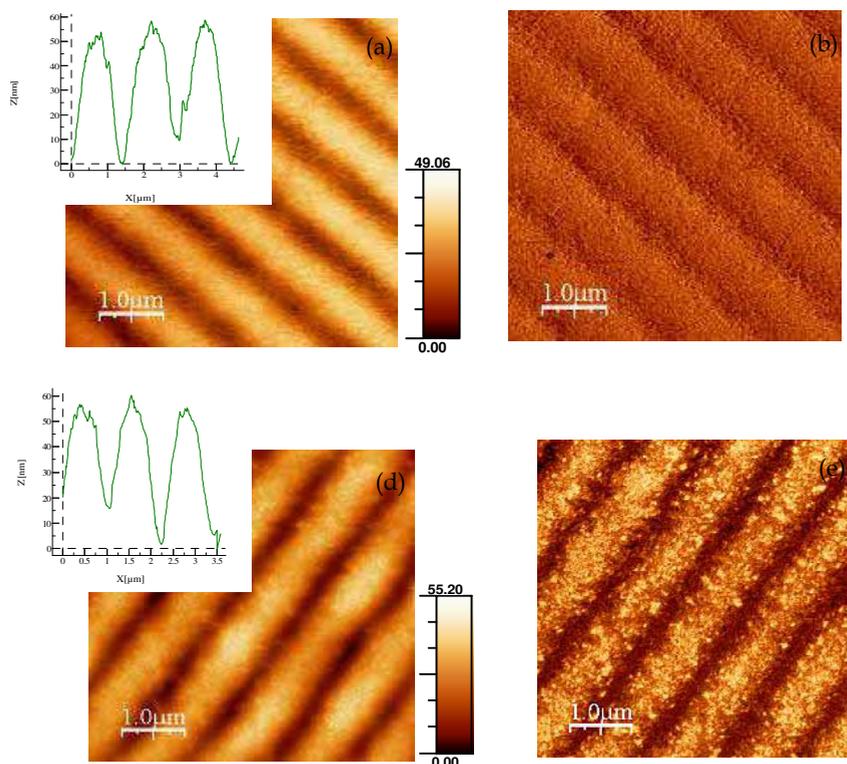

Fig. 5. AFM images obtained in tapping mode of holographic records without Ag⁺, (topography (a), phase (b), cross-section (inset)); and with Ag⁺, (topography (d), phase (e), cross-section (inset)) (Reprinted with permission from ref Balan et al., 2009. Copyright 2009 ACS)

The samples were disassembled before analysis and the free surface was kept for 24 h under vacuum to obtain a complete release of constraints stored in the polymer matrix.

Figures 5 a and b show the microstructures obtained at the surface of the sample containing no Ag^0. On the topographic image (figure 5 a), the grating can be clearly observed. The amplitude of the relief is ca. 50 nm (inset figure 5 a). This surface corrugation results from the difference in the polymer structure between the bright and dark areas of the incident interference pattern. Such a surface corrugation was already observed in other photopolymerizable systems (Jradi et al., 2008). The period measured by AFM corresponds exactly to the period of the interference pattern (1 µm).

In the case of Ag-doped material (figure 5 d, e), the grating was also clearly visible. The relief of the surface corrugation is of the same order as observed in the sample without nanoparticles, thus demonstrating that the polymer matrix is not significantly affected by

the presence of silver nanoparticles generated in situ. The contrast in the phase image is directly linked to difference in the polymer material structure. With the Ag-doped system, this contrast is more pronounced, meaning that the addition of Ag^+ favours the apparition of gradients in the polymer structure. This observation is in agreement with the higher diffraction efficiency linked to the addition of Ag^+. A close examination of the topography reveals a higher surface roughness in the case of the Ag-doped sample. The protuberances appearing in the phase image correspond to bright dots (figure 5 e); without hesitation, they can be attributed to silver nanoparticles since the mechanical interaction between the AFM tip and the metal nanoparticles emerging from the polymer surface is different than response on metal. Interestingly, the nanoparticules are not distributed homogeneously over the surface of the sample: Ag nanoparticles accumulate in the protruding regions of the grating. This spatial segregation is the key-factor accounting for the increase of holographic efficiency observed in doped samples.

SEM

Figure 6 shows micrographs recorded by scanning electron microscope (SEM) of two UV-cured samples obtained with Ag^+ and without Ag^+ respectively. Clearly, silver nanoparticles induce physical changes in the polymer (morphology, free volume) and chemical changes (local composition of the copolymer formed in the presence of nanoparticules (Yagci et al., 2008).

Presumably, the refractive index change results not only from the segregation of the nanoparticles but also from important changes in the structure of the polymer at the molecular scale.
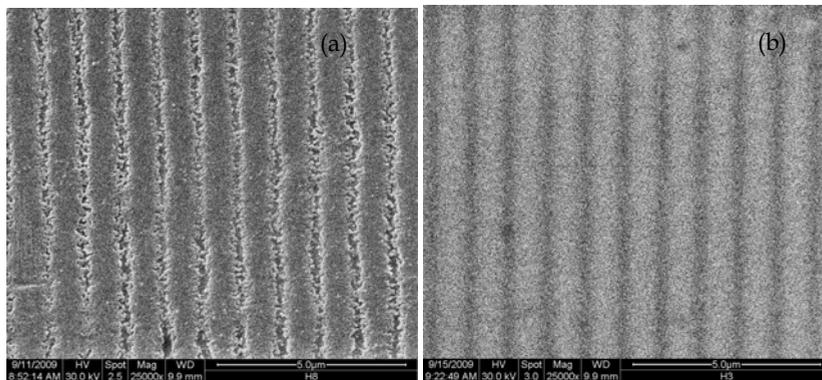

Fig. 6. SEM images of holographic records (a) without and (b) with 1% silver cations

TEM

TEM image (Figure 7), confirms without contest a patterned distribution of individual nanoparticles in the polymer matrix that form a grating with a period of ca 1 µm. As shown in Figure 7 particles are spherical with an average diameter of 20 nm.

3.3.2 Polymer tips terminated by silver nanowires for sensors

In this application, a one step photochemical process was used to generate a silver/polymer composite tip at the end of an optical fiber. Such an integrated nanodevice should achieve great success in the fields of plasmonic, nanoscale electronic devices or biomedical sensors.
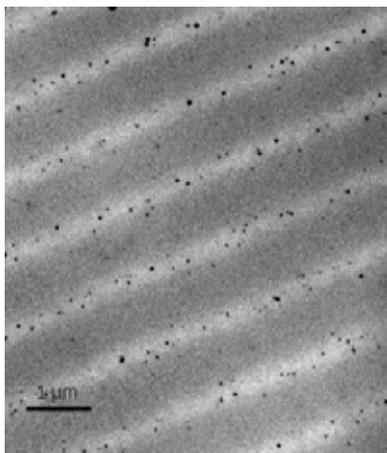
Fig. 7. TEM micrograph of the grating formed with silver nanoparticles

The simultaneous photo-reduction of silver and crosslinking photopolymerization involves amine-derived radicals generated from the reduction of the excited sensitizer in its triplet state by the electron-rich co-initiator molecules.

With a view to implementing at the end of optical fibers advanced optical functions that would take advantage of the unique properties of photogenerated metal nanoparticles, the reduction of silver cations was carried out using the light emerging from an optical fiber. The formulation developed for this purpose was sensitive to green laser light (typ. 532 nm).

The end of a freshly cleaved optical fiber was dropped into a formulation containing a photosensitizer (Eosin disodium salt, 0.5 % wt), a co-sensitizer (MDEA, 4 % wt), a silver salt ($AgNO_3$, 0.2 % wt) and a trifunctional monomer (PETA) (Jradi et al., 2010). Then, a green laser beam (532 nm) guided into the fiber was used to photo-reduce $Ag+$ cations; crosslinking photopolymerization involves amine-derived radicals generated from the reduction of the excited sensitizer in its triplet state by the electron-rich co-initiator molecules. As can be seen on figure 8, after careful solvent development, SEM analysis revealed the existence of silver nanowires bristling at the surface of the tip. The wires seemed to grow lengthwise from the top of the tip; their length ranged from 500 to 600 nm while their diameter was about 50 nm (see figure 8 c).

The mechanism of nanowires growth is still under investigation. However, the following points can be already considered for granted: silver nanoparticles located at the surface of the silver/polymer composite tips are prone to enhance the light field in their immediate vicinity and favour the nucleation and co-aggregation of silver nanoparticles that growth normally to the surface to generate silver nanowires. The anisotropic growth starts only from the small fraction of nanoparticles located at the polymer/solution interface and with such an orientation and size that the subsequent growth of the nanocrystaline structure is possible.

Of course, the great majority of metal nanoparticles, more or less deeply embedded in the polymer tip, do not meet these requirements, hence the low yield of nanowires. Because the surface plasmon field enhancement is higher in the regions corresponding to singularities, metal nanowires grow where the surface curvature is important. This process generates metal bumps at these sites, the tops of which form sharper and sharper singularities that amplify the anisotropy of the growing process. Therefore, the nanowires grow mainly lengthwise.
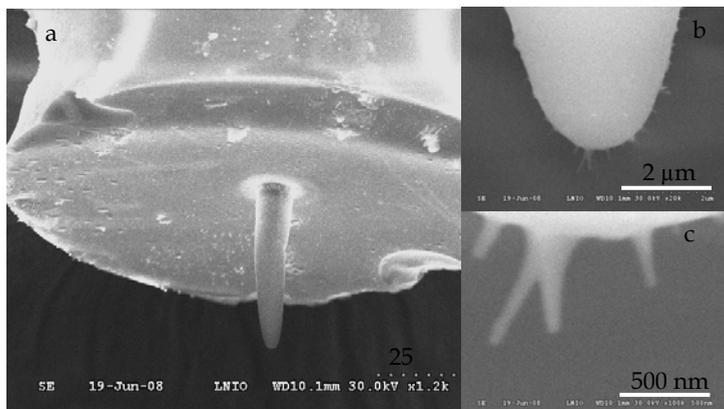
Fig. 8. Silver/polymer composite tip integrated at the end of an optical fiber and zooms of the extremity of the tip showing silver nanowires. Light Power = 2 µW, exposure time = 5s (Jradi et al., 2010. Copyright 2010 Nanotechnology)

The question of controlling their spatial distribution and orientation and providing an efficient anchoring of the nanowiers at the polymer surface remains unanswered. It can be observed that the new route used here leads to Ag nanowires perpendicular to the polymer surface. The nanowires are produced at the extremity of the polymer microtip, e.g. in the irradiated area.

Quite interestingly, electron beam irradiation generates no surface electrostatic effects on such composite polymer tips even up to 30 kV. The presence of silver nanoparticles in the composite improves its surface conduction. This feature is of the highest interest for applications in optical connecting and optical fiber sensing. In particular, metal nanowires that are one-dimensional (1D) objects have attracted particular interest, due to their unusual behaviour in the fabrication of nanoscale electronic devices and investigation of quantified conductance and biomedical nanoaddressing. Furthermore, such silver/polymer nanowires could be used as efficient nano-antenna probes for scanning-near field microscopy (Frey et al., 2002).

4. Conclusion

The works described in this chapter report on the use of photopolymerizable formulations that are capable of generating metal nanoparticles in situ and spatially control their distribution and orientation through photochemical activation. The process used avoids handling dry metal nanoparticles and aggregation that takes place during dispersion in a liquid formulation. Quite interestingly, the presence of metal nanoparticles was observed to accelerate and improve the crosslinking of multifunctional monomers forming the continuous polymer medium while the quantum yield of photobleaching of the sensitizer involved in the initiation process remained unaffected.

This system was used to record holographic gratings; it was observed that both the holographic sensitivity and the diffraction efficiency at maximum were significantly improved in the presence of particles. Obviously, the holographic efficiency of the photochemically assisted process depends on the coupling efficiency between the reaction generating nanoparticles and the photocuring of the polymerizable formulation. Electron

microscopy reveals the presence of straight strings of metal nanoparticles in the middle of bright fringes of the holographic pattern.

This photochemical process was also used to develop silver /polymer composite tips at the extremity of optical fibers. In a further approach aiming at generating a single metal nanoparticle at the top of a polymer tip ended optical fiber, attempts are made at increasing the non-linear character of the photochemical reaction used to create nanoparticles with the help of chemical additives.

This process provides a very powerful tool to manipulate nanoparticles at the nanoscale and offers a versatile means to fabricate microoptical elements, the design of which involves a patterning of the spatial distribution of nanoparticles. It opens up fascinating prospects in the field of microoptics and plasmonics.

5. References

Armelao, L.; Barreca, D.; Bottaro, G.; Gasparotto, A.; Gross, S.; Maragno, C. & Tondello, E. (2006). Recent trends on nanocomposites based on Cu, Ag and Au clusters: A closer look. *Coord. Chem. Rev.*, 250, 1294-1314

Aymonier, C.; Schlotterbeck, U.; Antonietti, L.; Zacharias, P.; Thomann, R.; Tiller, J. C. & Mecking, S. (2002). Hybrids of silver nanoparticles with amphiphilic hyperbranched macromolecules exhibiting antimicrobial properties. *Chem. Commun.*, 3018–3019

Balan, L.; Jin, M.; Malval, J-P.; Chaumeil, H.; Defoin, A. & Vidal, L. (2008). Fabrication of silver nanoparticle-embedded polymer promoted by combined photochemical properties of 2,7-diaminofluorene derivative dye. *Macromolecules*, 41, 9359-9365

Balan, L.; Schneider, R. & Lougnot, D. J. (2008). A new and convenient route to polyacrylate/silver nanocomposites by light-induced cross-linking polymerization. *Progress in Organic Coatings*, 62, 351-357

Balan, L.; Turck, C.; Soppera, O.; Vidal, L. & Lougnot, D. J. (2009). Holographic recording with polymer nanocomposites containing silver nanoparticles photogenerated in situ by the interference pattern. *Chem. Mater.*, 21 (24), 5711–5718

Balan, L.; Malval, J-P.; Schneider, R.; Le Nouen, D. & Lougnot, D. J. (2010). In situ fabrication of polyacrylate-silver nanocomposite through photoinduced tandem reactions involving eosin dye. *Polymer*, 51, 1363-1369

Carré, C. & Lougnot, D.J. (1990). Photopolymerisable material for recording in the 450–550 nm domain. *J Optics*, 21(3), 147-152

Collier, R. J.; Burckhardt, C. B. & Lin, L. H.; *Optical Holography*, Academic Press ; New York 1971

Corbierre, M. K.; Cameron, N. S.; Sutton, M.; Mochrie, S. G. J.; Lurio, L. B.; Ruhm, A. & Lennox, R. B. (2001). Polymer-stabilized gold nanoparticles and their incorporation into polymer matrices. *J Am.Chem. Soc.*, 123, 10411-10412

El-Sayed, M. A. (2001). Some interesting properties of metals confined in time and nanometer space of different shapes. *Acc. Chem. Res.*, 34, 257-264

Espanet, A.; Ecoffet, C. & Lougnot, D. J. (1999). PEW: Photopolymerization by evanescent waves . II - Revealing dramatic inhibiting effects of oxygen at submicrometer scale. *J Polym Sci A: Polym Chem.*, 37, 2075-2085.

Eustis, S. & El-Sayed, M. A. (2006). Why gold nanoparticles are more precious than pretty gold: Noble metal surface plasmon resonance and its enhancement of the radiative and nonradiative properties of nanocrystals of different shapes. *Chem. Soc. Rev.*, 35, 209–217

Fouassier, J-P. & Chesneau, E. (1991). Polymérisation induite sous irradiation laser visible, Le système éosine/photoamorceur ultra violet/amine. *Makromol. Chem.*, 192, 245-260

Frey, H. G.; Keilmann, F.; Kriele, A. & Guckenberger, R. (2002). Enhancing the resolution of scanning near-field optical microscopy by a metal tip grown on an aperture probe. *Appl. Phys. Lett.*, 81(26), 5030-5032

Goldenberg, L.M.; Sakhno, O.V.; Smirnova, T.N.; Helliwell, P.; Chechik, V. & Stumpe, J. (2008). Holographic Composites with Gold Nanoparticles: Nanoparticles Promote Polymer Segregation. *Chem. Mater.*, 20(14), 4619-4627 and references therein

Jin, R.C.; Cao, Y. W.; Mirkin, C. A.; Kelley, K. L.; Schatz, G. C. & Zheng, J. G. (2001). Photoinduced conversion of silver nanospheres to nanoplates. *Science*, 294, 1901-1903

Jradi, S.; Soppera, O. & Lougnot, D. J. (2008). Analysis of photopolymerized acrylic films by AFM in pulsed force mode. *J Microscopy*, 229, 151-161

Jradi, S.; Balan, L.; Zeng, X.H.; Plain, J.; Lougnot, D.J.; Royer, P.; Bachelot, R. & Soppera, O. (2010). Spatially controlled synthesis of silver nanoparticles and nanowires by photosensitized reduction. *Nanotechnology*, 21, 095605

Judeinstein, P.; Sanchez, C. (1996). Hybrid organic-inorganic materials : aland of multidisciplinarity. *J Mater. Chem.*, 6, 511-525

Kärkkäinen, A.H.O.; Tamkin, J.M.; Rogers, J. D.; Neal, D.R.; Hormi, O.E.; Jabbour, G.E.; Rantala, J.T. & Descour, M.R. (2002). Direct photolithographic deforming of organomodified siloxane films for micro-optics fabrication. *Applied Optics*, 41(19), 3988-3998

Kogelnik, H. (1969). Coupled wave theory for thick hologram gratings. Bell Syst. Tech. J., 48, 2909-2947

Korchev, A. S.; Bozack, M. J.; Slaten, B. L. & Mills, G. (2004). Polymer-initiated photogeneration of silver nanoparticles in SPEEK/PVA films: direct metal photopatterning. *J Am. Chem. Soc.*, 126, 10-11

Lougnot, D.J. & Turck, C. (1992). Photopolymers for holographic recording: III. Time modulated illumination and thermal post-effect. *Pure Appl. Opt.*, 1, 269-279

Lougnot, D.J. & Turck, C. (2002). Photopatterning of dry polymer films: on the relative involvement of diffusive and capillary convection in the self-corrugation process. *Helv. Chim.. Acta,* 85, 115-134

Mandal, T.K.; Fleming, M. S. & Walt. D.R. (2002). Preparation of polymer coated gold nanoparticles by surface confined living radical polymerization at ambient temperature. *Nano Lett.*, 2, 3-7

Mehnert, R.; Pincus, A.; Janorsky, I.; Stowe, R. & Berejka, A. In Chemistry & Technology of UV & EB Formulation for Coatings, Inks & Paints; SITA Technology Ltd.: London, 1997, p 217

Mikhailov, V.; Wurtz, G.A.; Elliot, J.; Bayvel, P. & Zayats, A.V. (2007). Dispersing light with surface plasmon polaritonic crystals. *Phys. Rev. Lett.*, 99, 83901

Nakamura, T.; Nozaki, J.; Tomita, Y.; Ohmori, K. & Hidaka, M. (2009). Holographic recording sensitivity enhancement of ZrO2 nanoparticle–polymer composites by hydrogen donor and acceptor agents. *J Optics A: Pure and Applied Optics* 11(2), 024010/1

Noiret, N.; Meyer, C. & Lougnot D. J. (1994). Photopolymers for holographic recording. V. Self-processing systems with near infrared sensitivity. *Pure Appl. Opt.*, 3, 55-71

Pyszka, I. & Kucybała, Z. (2008). The effect of co-initiator structure on photoinitiating efficiency of photoredox couples composed of quinoline[2,3-b]-1H-imidazo[1,2-a]pyridinium bromide and phenoxyacetic acid or N,N-dimethylaniline derivatives. *Polym. Bull.*, 61, 553-562

Sakamoto, M.; Tachikawa, T.; Fujitsuka, M. & Majima, T. (2007). Photochemical Formation of Au/Cu Bimetallic Nanoparticles with Different Shapes and Sizes in a PVA Film. *Adv. Funct. Mater.*, 17, 857-862

Sakamoto, M.; Fujistuka, M. & Majima, T. (2009). Light as a construction tool of metal nanoparticles: Synthesis and mechanism. *J Photochem and Photobiol C: Photochem Reviews* 10(1) 33-56

Samui, A. B. (2008). Holographic recording medium. *Recent Patents on Materials Science*, 1, 74

Sanchez, C.; Escuti, M.; Heesh, C.; Bastiaansen, C.; Broer, D.; Loos, J. & Nussbaumer, R. (2005). TiO2 Nanoparticle–Photopolymer Composites for Volume Holographic Recording. *Adv. Funct. Mat.*, 15, (10), 1623-1629

Sangermano, M.; Yagci, Y. & Rizza, G. (2007). In Situ Synthesis of Silver-Epoxy Nanocomposites by Photoinduced Electron Transfer and Cationic Polymerization Processes. *Macromolecules*, 40, 8827-8829

Shenhar, R. & Rotello, V. M. (2003). Nanoparticles: Scaffolds and Building Blocks. *Acc. Chem. Res.* 36, 549-561

Sondi I. & Salopek-Sondi B. (2004). Silver nanoparticles as antimicrobial agent: a case study on E. coli as a model for Gram-negative bacteria. *Journal of Colloid and Interface Science*, 275, 177–182

Soppera, O. & Croutxé-Barghorn, C. (2003). Real-time Fourier transform infrared study of free-radical UV-induced polymerization of hybrid sol–gel. I. Effect of silicate backbone on photopolymerization kinetics. *J Poly. Sci. Part A: Poly. Chem.*, 41(5), 716–724

Stranik, O.; Iacopino, D.; Nooney R.; McDonagh, C. & MacCraith, B. D. (2010). Optical Properties of Micro-patterned Silver Nanoparticle Substrates. *J Fluoresc.*, 20, 215– 223

Sudeep, P. K. & Kamat, P. V. (2005). Photosensitized Growth of Silver Nanoparticles under Visible Light Irradiation: A Mechanistic Investigation. *Chem. Mater.*, 17, 5404-5410

Tizazu, G.; Adawi, A. M.;. Leggett, G. J. & Lidzey, D. G. (2009). Photopatterning, Etching, and Derivatization of Self-Assembled Monolayers of Phosphonic Acids on the Native Oxide of Titanium. *Langmuir*, 25 (18), 10746–10753

Ung, T.; Liz-Marzàn L. M. & Mulvaney, P. (2001). Optical properties of thin films of Au@SiO2 particles. *J Phys. Chem. B*, 105, 3441-3452

Vaia, R.A.; Dennis, C.L.; Natarajian, L.V.; Tondiglia, V.P.; Tomlin, D.W. & Bunning, T.J. (2001). One-Step, Micrometer-Scale Organization of Nano- and Mesoparticles Using Holographic Photopolymerization: A Generic Technique. *Adv. Mater.*, 23, 1570- 1574

Vriezema, D.M.; Comellas-Aragones, M.; Elemans, J.A.A.W.; Cornelissen, J.J.L.M.; Rowan, A.E. and Nolte, R.J.M. (2005). Self-Assembled Nanoreactors. *Chem. Rev.* 105,1445-1490

Wang, X.; Naka, K.; Itoh, H.; Park, S. & Chujo, Y. (2002). Synthesis of silver dendritic nanostructures protected by tetrathiafulvalene. *Chem. Commun.*, 1300-1301

Yagci, Y.; Sangermano, M. & Rizza G. (2008). In situ synthesis of gold-cross-linked poly(ethylene glycol) nanocomposites by photoinduced electron transfer and free radical polymerization processes. *ChemComm.*, 2771-2773.

Yagci, Y.; Sangermano, M. & Rizza, G. (2008). A visible light photochemical route to silver–epoxy nanocomposites by simultaneous polymerization–reduction approach. *Polymer*, 49, 5195-5198
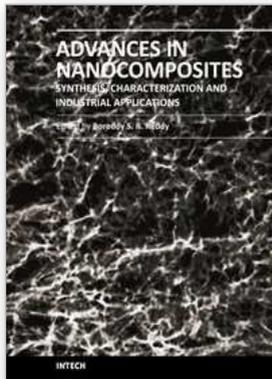
Advances in Nanocomposites - Synthesis, Characterization and Industrial Applications
Edited by Dr. Boreddy Reddy

ISBN 978-953-307-165-7
Hard cover, 966 pages
Publisher InTech
Published online 19, April, 2011
Published in print edition April, 2011

Advances in Nanocomposites - Synthesis, Characterization and Industrial Applications was conceived as a comprehensive reference volume on various aspects of functional nanocomposites for engineering technologies. The term functional nanocomposites signifies a wide area of polymer/material science and engineering, involving the design, synthesis and study of nanocomposites of increasing structural sophistication and complexity useful for a wide range of chemical, physicochemical and biological/biomedical processes. "Emerging technologies" are also broadly understood to include new technological developments, beginning at the forefront of conventional industrial practices and extending into anticipated and speculative industries of the future. The scope of the present book on nanocomposites and applications extends far beyond emerging technologies. This book presents 40 chapters organized in four parts systematically providing a wealth of new ideas in design, synthesis and study of sophisticated nanocomposite structures.

How to reference

In order to correctly reference this scholarly work, feel free to copy and paste the following:

Lavinia Balan and Daniel-Joseph Lougnot (2011). Photochemically Implemented Metal/Polymer Nanocomposite Materials for Advanced Optical Applications, Advances in Nanocomposites - Synthesis, Characterization and Industrial Applications, Dr. Boreddy Reddy (Ed.), ISBN: 978-953-307-165-7, InTech, Available from: http://www.intechopen.com/books/advances-in-nanocomposites-synthesis-characterization-and-industrial-applications/photochemically-implemented-metal-polymer-nanocomposite-materials-for-advanced-optical-applications

INTECH
open science | open minds